

# Effects of Anthocyanin Extracts from Bilberry (*Vaccinium myrtillus* L.) and Purple Potato (*Solanum tuberosum* L. var. 'Synkeä Sakari') on the Plasma Metabolomic Profile of Zucker Diabetic Fatty Rats

Kang Chen,<sup>†</sup> Xuetao Wei,<sup>†</sup> Jian Zhang, Raghunath Pariyani, Johanna Jokioja, Maaria Kortensniemi, Kaisa M. Linderborg, Jari Heinonen, Tuomo Sainio, Yumei Zhang,\* and Baoru Yang\*



Cite This: <https://dx.doi.org/10.1021/acs.jafc.0c04125>



Read Online

ACCESS |



Metrics & More



Article Recommendations



Supporting Information

**ABSTRACT:** This study compared the effects of the nonacylated and acylated anthocyanin-rich extracts on plasma metabolic profiles of Zucker diabetic fatty rats. The rats were fed with the nonacylated anthocyanin extract from bilberries (NAAB) or the acylated anthocyanin extract from purple potatoes (AAPP) at daily doses of 25 and 50 mg/kg body weight for 8 weeks. <sup>1</sup>H NMR metabolomics was used to study the changes in plasma metabolites. A reduced fasting plasma glucose level was seen in all anthocyanin-fed groups, especially in the groups fed with NAAB. Both NAAB and AAPP decreased the levels of branched-chain amino acids and improved lipid profiles. AAPP increased the glutamine/glutamate ratio and decreased the levels of glycerol and metabolites involved in glycolysis, suggesting improved insulin sensitivity, gluconeogenesis, and glycolysis. AAPP decreased the hepatic *TBC1D1* and *G6PC* messenger RNA level, suggesting regulation of gluconeogenesis and lipogenesis. This study indicated that AAPP and NAAB affected the plasma metabolic profile of diabetic rats differently.

**KEYWORDS:** acylated anthocyanins, nonacylated anthocyanins, Zucker diabetic fatty rats, type 2 diabetes, NMR metabolomics

## INTRODUCTION

Diabetes compromises the quality of life and brings about a substantial economic burden to the society. Approximately 90% of the diabetic patients have type 2 diabetes characterized by peripheral insulin resistance and a decrease in the number and activity of pancreatic  $\beta$ -cells.<sup>1</sup> Healthy food choices are important for reducing the risk of metabolic syndromes and type 2 diabetes. Phenolic compounds have been shown to affect key pathways of carbohydrate metabolism and hepatic glucose (GLU) homeostasis including glycolysis, glycogenesis, and gluconeogenesis, which are usually impaired in diabetes.<sup>2</sup> As a major group of phenolic compounds in the diet, anthocyanins have potential in lowering the risk for the development of various chronic diseases because of their role in regulating energy metabolism as well as anti-inflammatory and antioxidative effects.<sup>3</sup> Furthermore, anthocyanins inhibit the activities of  $\alpha$ -glucosidase and pancreatic  $\alpha$ -amylase, which is also the target of action by some antidiabetic drugs such as acarbose to reduce the digestion and absorption of carbohydrates.<sup>2</sup>

Dietary anthocyanins are absorbed as an intact glycoside or after hydrolysis to aglycones by lactate phlorizin hydrolase before absorption by enterocytes. The absorbed glycosides and aglycones undergo metabolism by phase I and phase II enzymes, resulting in methylation, glucuronidation, and sulfatation, and the resulting metabolites are excreted *via* urine. The absorption of anthocyanins, either as intact glycosides or as aglycones, is low in the small intestine.<sup>4</sup> The unabsorbed anthocyanins are converted by the action of gut microbiota to phenolic acids, which are further absorbed into

the circulation.<sup>4</sup> The metabolites of anthocyanins modulate the gut microbiota and production of short-chain fatty acids.<sup>5</sup> Although most of the data have been obtained on the metabolism of nonacylated anthocyanins from fruits and berries, there has been little research focusing on the metabolism of acylated anthocyanins, which are commonly found in red and purple potatoes as well as dark-colored vegetables such as purple cabbages and purple carrots.<sup>6</sup> In acylated anthocyanins, the sugar residues are acylated with organic acids, commonly caffeic, *p*-coumaric, ferulic, sinapinic, and malonic acids.<sup>7</sup> The acylation process of anthocyanins in plants is catalyzed by anthocyanin acyltransferases (ACTs), which have high substrate specificity for both the anthocyanin acceptors and the acyl group donors. In plants, there are mainly two types of ACTs that are classified based on the acyl group donors: the BAHD family using acyl-CoA and the serine carboxypeptidase-like group using acyl-activated sugar.<sup>8</sup>

Acylation alters the physical and chemical properties of anthocyanins, and acylated anthocyanins have been reported to be more resistant to higher pH, heat, and light<sup>9</sup> and to have higher antioxidant activity<sup>10</sup> than the corresponding nonacylated anthocyanins. The higher stability of acylated anthocyanins is likely to result from the intramolecular

Received: June 30, 2020

Revised: August 10, 2020

Accepted: August 10, 2020

Published: August 10, 2020

stacking of the acyl groups with the pyrylium ring, reducing the susceptibility of nucleophilic attack of water.<sup>7</sup> *In vitro*, acylated anthocyanins with higher stability have shown more potent inhibitory activity on  $\alpha$ -glucosidase compared to nonacylated anthocyanins.<sup>11</sup> Although *in vitro* studies using the gastrointestinal model indicated higher bioavailability of acylated anthocyanins from purple sweet potatoes than nonacylated anthocyanins from red wines,<sup>12</sup> acylated anthocyanins in purple carrots showed an 8–14-fold decrease in anthocyanin recovery in both urine and plasma compared to their nonacylated counterpart in a bioavailability study in humans.<sup>13</sup> Both the acylation pattern and plant matrix play a role in the absorption and bioavailability of anthocyanins. Furthermore, the fermentable property of anthocyanins in the gut might exert beneficial effects on human health.<sup>14</sup> Currently, little information is available about the possible differences in biological functions *in vivo* between acylated and nonacylated anthocyanins. Based on a dietary survey of 36,037 individuals in 10 European countries, the daily intake of anthocyanins ranges from 18.73 to 64.88 mg and the major sources of anthocyanins were fruits and wine.<sup>15</sup> Increasing consumption of dark-colored potatoes and vegetables could be a more affordable and effective way for increasing the dietary intake of anthocyanins. Potato is a globally major agricultural crop, and potatoes are consumed as staple food across the world. Red- and purple-colored potatoes are widely cultivated in South America, Asia, Europe, and North America. Because of the high yield and low production cost, potatoes represent sustainable sources of anthocyanins, which can also be used as functional ingredients in food and nutraceuticals.

Understanding how the acylated and nonacylated anthocyanins affect metabolic homeostasis in type 2 diabetes is important for understanding their role in the management of the disease. Metabolomics has emerged as a powerful tool for metabolite profiling in the field of pharmacology, disease research, and toxicology as well as nutrition and food sciences. Indeed, nuclear magnetic resonance (NMR) metabolomics is a reproducible and high-throughput method for elucidating the metabolic state and potential changes in the metabolic pathways.<sup>16</sup> A range of metabolites detectable by metabolomics have been indicated as potential biomarkers associated with different stages of type 2 diabetes in humans.<sup>1</sup>

NMR metabolomics has been applied to investigate the long-term use of drugs on the metabolism of patients as well as in nutritional metabolomics to study the metabolic impact of different dietary patterns. NMR metabolomics revealed that administration of metformin for 18 months altered the circulating level of alanine and aromatic amino acids in patients with coronary disease.<sup>17</sup> The NMR metabolomic study of urine samples has proven to be useful in the assessment of exposure to diet of different glycemic indexes and dietary intake of fibres.<sup>18</sup> To our best knowledge, no research has been reported on the metabolomic impact of anthocyanins on type 2 diabetes in humans or animal models.

In the current study, we aimed to investigate and compare the impact of acylated anthocyanins from purple potatoes (*Solanum tuberosum* L.) and nonacylated anthocyanins from bilberries (*Vaccinium myrtillus* L.) on the metabolic status of Zucker diabetic fatty (ZDF, *fa/fa*) rats as an animal model of type 2 diabetes. Metabolic changes in ZDF rats were compared to their lean counterparts using NMR metabolomics to find possible changes of the potential metabolic biomarkers of type 2 diabetes. We hypothesized that there is a different impact

between the nonacylated anthocyanin extract from bilberries (NAAB) and the acylated anthocyanin extract from purple potatoes (AAPP) on the diabetic metabolic state in ZDF rats.

## MATERIALS AND METHODS

**Extraction, Purification, and Analysis of Anthocyanins from Bilberries and Purple Potatoes.** Certified organic fresh bilberries (*V. myrtillus* L.), collected from the Kainuu region, Finland, were purchased from Pakkasmarja Oy (Suonenjoki, Finland). Purple potatoes (*S. tuberosum* L.) of the cultivar 'Synkeä Sakari' were provided by Clanet Oy (Espoo, Finland). The potatoes were cultivated and harvested in 2017 in the Lohja area, Finland, sliced, and freeze-dried before extraction. Anthocyanins were extracted with 70% v/v aqueous ethanol containing 2% v/v acetic acid using a solid–liquid ratio of 1:5 (w/v). The extraction was repeated three times, and the extracts were combined and filtered, followed by vacuum evaporation to remove ethanol. After evaporation, each of the extracts was loaded onto a column packed with an equilibrated Amberlite XAD-16 (Sigma-Aldrich, Steinheim, Germany) adsorbent for purification. After loading, the column was first washed with purified water to elute the sugars and organic acids, after which anthocyanins were eluted with ethanol. The eluent was collected and subjected to vacuum rotary evaporation to remove ethanol. After evaporation, the extracts were lyophilized and stored at  $-80$  °C until analysis.

The composition and content of anthocyanins and other phenolic compounds in the extracts were analyzed with high-performance liquid chromatography (HPLC) with diode-array detection (HPLC-DAD) and high-resolution UHPLC-ESI(+)-Q-ToF-MS using the methods reported in our previous study.<sup>19</sup> Three replicate samples of each extract were dissolved with MeOH/HCl 99/1 and filtrated (0.45  $\mu$ m, PTFE; VWR, Radnor, PA). An absorption maximum at 520 nm was used for detecting anthocyanins and those at 354 and 320 nm for flavonol glycosides and hydroxycinnamic acids, respectively. For quantification, anthocyanins were calculated as cyanidin-3-*O*-glucoside equivalents (Extrasynthese, Genay, France). Flavonol glycosides were quantified as quercetin-3-*O*-rutinoside equivalents (Extrasynthese, Genay, France). Hydroxycinnamic acids were calculated as caffeic acid equivalents (Sigma-Aldrich, St Louis, MO).

**Animals and Feeding.** In this study, male ZDF rats were used to evaluate the metabolic impact of anthocyanins from purple potatoes and bilberries. Lean Zucker rats (*fa/+*) were used as healthy controls. All experimental protocols were approved by the Institutional Animal Ethics Committee of Peking University (no. LA2016285) and carried out in compliance with the OECD 408 guideline for the care and use of laboratory animals.

Male ZDF and lean Zucker rats of 3 weeks old were purchased from Beijing Vital River Laboratory Animal Technology Co., Ltd. (Beijing, China). The rats were maintained in a specific pathogen-free environment at the Animal Housing Unit of Peking University (Beijing, China) under controlled temperature (23–25 °C) and a 12 h light/12 h dark cycle. After 1 week of adaptation, the ZDF rats were randomly divided into five groups, with eight rats in each group, receiving 8 weeks of daily feeding as follows: (1) ZDF rats fed with high-fat diet Purina#5008 (Table S1)<sup>20</sup> and NAAB providing a daily dosage of 50 mg/kg body weight (high-dose NAAB, H-NAAB); (2) the ZDF rats fed with Purina#5008 diet and AAPP providing a daily dosage of 50 mg/kg body weight (high-dose AAPP, H-AAPP); (3) the ZDF rats fed with Purina#5008 diet and NAAB providing a daily dosage of 25 mg/kg body weight (low-dose NAAB, L-NAAB); (4) the ZDF rats fed with Purina#5008 diet and AAPP providing a daily dosage of 25 mg/kg body weight (low-dose AAPP, L-AAPP); and (5) ZDF rats fed only with Purina#5008 diet as the diabetic model group (M). The lean Zucker rats were divided into two groups, one fed with normal diet (ND,  $n = 8$ ) and the other with high-fat Purina#5008 diet as the control group (Con,  $n = 8$ ). During the feeding with different diets, all rats were kept in separate cages, and the anthocyanin extracts were given by gavage. The dosages of anthocyanin extracts were chosen based on the dosages used in previous animal<sup>21</sup> and human<sup>22</sup> studies. The anthocyanin content in the extracts was taken into

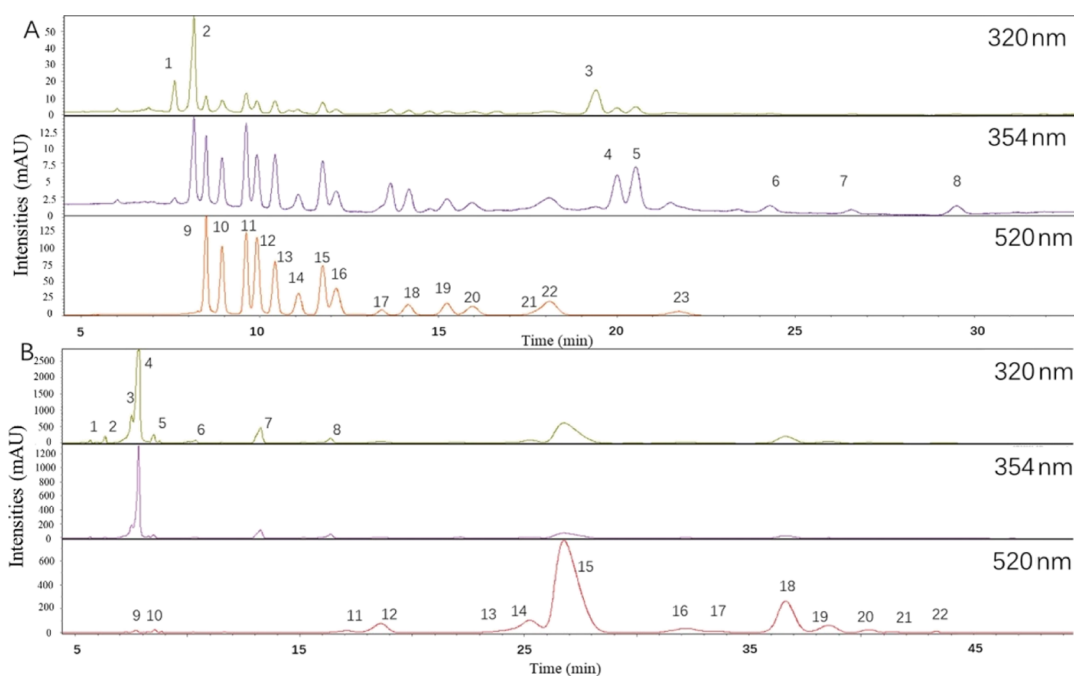


**Figure 1.** HPLC-DAD chromatograms of the anthocyanin extracts showing anthocyanins (520 nm), flavonol glycosides (354 nm), and hydroxycinnamic acids (320 nm) from bilberries (*V. myrtillus* L.) (A) and purple potato (*S. tuberosum* L. 'Synkeä Sakari') extracts (B). Numbering of the peaks refers to Table 1.

account when determining the amount of the extracts given to the rats in the anthocyanin-treated groups. The feed supply was replaced once in every 2 days to prevent oxidization of the fats in diets. Feed and water intake on the 30th and 60th day were monitored. The weekly feed intake and body weight were recorded. After 8 weeks of intervention, the rats were sacrificed under isoflurane anesthesia after overnight fasting. Plasma samples were collected by centrifuging the blood samples at 3000g for 10 min at 4 °C. The plasma samples were stored at −80 °C until analyses.

**Biochemical Assays.** The plasma concentrations of aspartate transaminase (AST), alanine aminotransferase (ALT), triglyceride (TG), total protein (TP), albumin (ALB), blood urea nitrogen (BUN), and GLU were measured by using a Hitachi 7170A/7180 Biochemical Analyzer (Hitachi, Japan). The plasma insulin level was determined with an ELISA kit (Beyotime Biotechnology, China).

**<sup>1</sup>H NMR Spectroscopic Analysis.** An aliquot of 220 μL of plasma was mixed with 440 μL of the phosphate buffer (90 mmol/L NaH<sub>2</sub>PO<sub>4</sub>, pH = 7.4) containing 15% D<sub>2</sub>O to minimize variations in pH. After vortexing, the samples were centrifuged at 12,000g for 10 min at 4 °C to separate the precipitates. Aliquots of 600 μL of the resulting supernatants were transferred into 5 mm NMR tubes. The NMR experiments were performed at 298 K using a 600 MHz Bruker AVANCE III NMR spectrometer (Bruker BioSpin AG, Fällanden, Switzerland) equipped with a Prodigy TCI cryoprobe and a precooled SampleJet sample changer. One-dimensional <sup>1</sup>H NMR spectra were recorded from all the plasma samples using the Carr–Purcell–Meiboom–Gill (CPMG) pulse sequence. The parameters used for the one-dimensional (1D) CPMG pulse sequence were as follows: spectral sweep width, 16.02 ppm; data points, 64 K; flip angle of radio frequency pulse, 90°; total relaxation delay, 5 s. T2 filtering was obtained with an echo time of 2 ms repeated 64 times, resulting in a total duration of effective echo time of 256 ms, and the number of scans was 128. All the spectra were manually phase- and baseline-corrected with Topspin 3.5 software (Bruker BioSpin GmbH, Rheinstetten, Germany). The chemical shift of α-GLU (δ = 5.23 ppm) was used to align the spectra.

**Metabolite Identification.** Metabolites were identified based on 1D CPMG NMR chemical shifts reported in the literature, Chenomx NMR Suite 7.5 software (Chenomx Inc., Edmonton, Alberta, Canada) and the metabolite database Human Metabolome Database (HMDB,

<http://www.hmdb.ca>). The identification was further confirmed by two-dimensional (2D) <sup>1</sup>H–<sup>13</sup>C heteronuclear single-quantum correlation spectroscopy (HSQC), <sup>1</sup>H–<sup>1</sup>H correlation spectroscopy (COSY), and *J*-resolved spectroscopy (JRES).

#### Measurement of the Gene Expression of *G6PC* and *TBC1D1*.

Total RNA from the liver was isolated using a TransZol Up kit (Transgen biotech, Beijing, China) according to the manufacturer's directions. The RNAs (1.0 μg) were reverse-transcribed to complementary DNA (cDNA) using a TransScript One-step gDNA Removal and cDNA Synthesis SuperMix (TransGen Biotech, Beijing, China). The expression level of *G6PC* and *TBC1D1* genes in rat livers was measured by quantitative real-time-polymerase chain reaction (PCR). The primer sequences were as follows: *G6PC*: forward primer CGTCACCTGTGAGACTGGAC, reverse primer GCCCAG-TATCCCAACCACAA; *TBC1D1*: forward primer TCGATGACACCTTCGCCAAA, reverse primer TGGCCAATCGTGAAGAG-CAT.

**Statistical Analysis.** A total of 46 plasma samples out of 56 plasma samples were included for <sup>1</sup>H NMR spectroscopic analysis (M, *n* = 6; L-NAAB, *n* = 6; L-NAAB, *n* = 7; L-AAPP, *n* = 6; H-AAPP, *n* = 6; CON, *n* = 7; ND, *n* = 8) because an insufficient quantity of plasma was obtained from some animals and excluding three rats with an extremely high ketone level (determined as 2.5 × standard deviations outside of the mean). These rats were therefore excluded from the analysis. The 1D <sup>1</sup>H NMR spectra of plasma were binned into 0.01 ppm integral regions using the Chenomx NMR software suite (Professional edition, version 8.3, Chenomx, Edmonton, AB, Canada), and the water region (4.70–4.95 ppm) was removed. Data are Pareto-scaled before multivariate data analysis using SIMCA-P+ (V12.0, Umetrics AB, Umeå, Sweden). The relative concentration of the metabolites was determined based on the binned area. Bins used for relative quantification are specified in Table S2. Correlation analysis and pathway analysis were performed using the MetaboAnalyst platform based on high-quality KEGG metabolic pathways. The Kolmogorov–Smirnov test was used to check the normality of the data distribution in GraphPad Prism V 6.0 (GraphPad Software Inc., San Diego, USA). If data were normally distributed, a parametric one-way analysis of variance (ANOVA) was performed; otherwise, the nonparametric Kruskal–Wallis test was applied, and post hoc Fisher's LSD test or Dunn's test was applied between groups.



Statistical significance between groups was assessed at levels \* $p < 0.05$ , \*\* $p < 0.01$ , and \*\*\* $p < 0.001$ .

## RESULTS

### Identification and Quantification of Anthocyanins.

Anthocyanins, flavonol glycosides, and hydroxycinnamic acids from bilberry and purple potato extracts were identified and quantified by UHPLC-ESI(+)-Q-ToF-MS and HPLC-DAD. The HPLC chromatograms are presented in Figure 1, showing anthocyanins, flavonol glycosides, and phenolic acids at different wavelengths. Table 1 consists of information related to the identification of the peaks including MS fragments and the accurate masses of the molecular ions of the peaks. NAAB were nonacylated. Each gram of NAAB contained  $423.89 \pm 7.02$  mg of anthocyanins,  $14.96 \pm 0.54$  mg of flavonol glycosides, and  $19.30 \pm 0.39$  mg of hydroxycinnamic acids with chlorogenic acid being the dominant. Each gram of AAPP contained  $248.74 \pm 7.14$  mg of anthocyanins and  $144.07 \pm 4.21$  mg of hydroxycinnamic acids consisting of mostly chlorogenic acid, while no flavonol glycosides were detected in AAPP. The anthocyanins of NAAB consisted of mostly glucosides, galactosides, and arabinosides of delphinidin, petunidin, cyanidin, peonidin, and malvidin. AAPP contained only acylated anthocyanins, with petunidin-coumaryl-rutinoside-glucoside ( $160.82 \pm 4.39$  mg/g) as the dominating compound, followed by peonidin-coumaryl-rutinoside-glucoside ( $40.30 \pm 2.23$  mg/g) and petunidin-caffeoyl-rutinoside-glucoside ( $12.31 \pm 0.26$  mg/g) (Table 1). The total anthocyanin content in the extracts ( $423.89$  mg/g for the bilberry extract and  $248.74$  mg/g for the potato extract) was taken into account when determining the daily dosage in the feeding of the experimental rats.

### Intake of Feed and Water as Well as Body Weight.

Metabolic cage was used to monitor the intake of feed and water on the 30th day and the 60th day of the intervention. Figure 2A,B shows that the diabetic ZDF rats fed with high-fat diet (M) had higher daily intake of water and feed on the 30th day ( $p < 0.001$ ,  $p < 0.001$ ) and the 60th day ( $p < 0.001$ ,  $p < 0.001$ ) of the intervention compared to the lean Zucker rats fed with ND or high-fat diet (Con). In the groups treated with anthocyanin extracts (L-NAAB, H-NAAB, and H-AAPP), the water intake was significantly decreased on the 30th day ( $p < 0.05$ ,  $p < 0.05$ , and  $p < 0.001$ ) compared to that in the M group. The L-NAAB group also showed decreased water intake on the 60th day ( $p < 0.05$ ). Compared to the M group, the H-AAPP group showed a significant decrease in feed intake on both the 30th day ( $p < 0.001$ ) and 60th day ( $p < 0.01$ ). Overall, a decrease was seen in weekly feed intake in all treatment groups in the late period of intervention in comparison with the model (M) group, with the reduction being statistically significant in the H-NAAB and H-AAPP groups at the 8th week (Figure 2C).

As illustrated in Figure 2D, the M group showed a significant increase in body weight compared to both the ND and Con groups, highlighting the impact of the leptin gene deficiency ( $p < 0.001$ ,  $p < 0.001$ ). There were no significant differences in body weight between the anthocyanin-fed groups and the M group.

**Biochemical Assays.** The M group showed clearly different biochemical profiles of plasma compared to the lean Zucker rats of the Con and ND groups (Table 2), characterized by lower levels of aspartate transaminase (AST) and higher levels of TP, BUN, triglyceride (TG), and

GLU. Groups fed with the nonacylated anthocyanin extracts (L-NAAB and H-NAAB) showed significantly decreased fasting plasma GLU levels ( $p < 0.01$ ,  $p < 0.001$ ) compared to the rats in the model (M) group fed with the same diet without the anthocyanin extract. The groups fed with the acylated anthocyanin extracts (L-AAPP and H-AAPP) also showed decreased levels of plasma GLU, but the difference did not reach statistical significance. No statistically significant difference was found in insulin levels in fasting plasma among the groups at the end of treatment period (Table 2).

**Hepatic mRNA Level of G6PC and TBC1D1.** The hepatic messenger RNA (mRNA) levels of *G6PC* and *TBC1D1* genes are shown in Figure S1. The M group showed the highest level of hepatic *G6PC* gene expression, which was significantly decreased in the groups fed with the potato anthocyanin extract (L-AAPP:  $p < 0.01$ ; H-AAPP:  $p < 0.05$ ). The qPCR analysis showed a decrease in the level of mRNA of *TBC1D1* in the group treated with H-AAPP compared to the model group ( $p < 0.01$ ), indicating a reduction in hepatic *TBC1D1* gene expression.

**<sup>1</sup>H NMR Spectra of Plasma Samples.** Representative CPMG spectra of plasma samples are shown in Figure 3A. Altogether, 26 metabolites were identified using Chenomx and 2D NMR (Figures S2–S4.), and their chemical shifts and peak multiplicity are summarized in Table S3.

**Alterations in the Metabolomic Profile in ZDF Rats.** OPLS-DA and their loading S line plot were performed between the M group and the Con or ND group (Figure 3B,C) to investigate the metabolite alterations associated with the leptin gene deficiency and the influence of the high-fat diet and thereby to pinpoint the potential biomarkers in type 2 diabetes and to verify the induction of diabetes.

The goodness-of-fit and predictability for the OPLS-DA models were reflected by the values of  $R^2Y_{(cum)} = 0.988$  and  $Q^2Y_{(cum)} = 0.967/R^2Y_{(cum)} = 0.995$  and  $Q^2Y_{(cum)} = 0.977$ . A CV-ANOVA value of  $3.90095e^{-005}/1.04925e^{-006}$  and 100 times permutation tests ( $Y$ -intercepts:  $R^2 = 0.286$ ,  $Q^2 = -0.448/R^2 = 0.297$ ,  $Q^2 = -0.468$ ) confirmed the validity of the models (Figure S5A,B).

In the corresponding loading S line plot, metabolite variations were distinguished according to the value of correlation coefficients, where a red signal indicated more significant contribution to the class separation than a green one. The negative side of the loading plot constituted metabolites increased in the M group including lipids ( $\delta$  0.80–0.90, etc.), branched-chain amino acids (BCAAs) (leucine,  $\delta$  0.96–0.97; isoleucine,  $\delta$  1.00; valine,  $\delta$  0.98–0.99), lactate ( $\delta$  1.31–1.33, 4.10–4.13), alanine ( $\delta$  1.47–1.49), acetone ( $\delta$  2.22), pyruvate ( $\delta$  2.37), citrate ( $\delta$  2.52–2.56), glycerol ( $\delta$  3.64–3.66), unsaturated lipids ( $\delta$  5.27–5.37), GLU ( $\delta$  4.62–4.67, 5.22–5.24), and creatine/creatinine ( $\delta$  3.04), whereas the positive side constituted metabolites decreased in the M group (glutamine,  $\delta$  2.43–2.47). Metabolites mentioned above were major compounds responsible for the separation between nondiabetic groups and diabetic groups. In addition, the content of glycine was significantly lower in the M group compared to that in the ND group, whereas no such difference was found between the M and Con groups. In addition to fat content, the feed composition (Table S1) of the high-fat diet (the M, Con, and anthocyanin-treated groups) and the ND also differed in the content of other nutrients such as amino acids and minerals, which could possibly have an impact on the energy

**Table 1. Identification and Quantification of Anthocyanins, Flavonol Glycosides, and Hydroxycinnamic Acids in NAAB and AAPP Based on HPLC-DAD and High-Resolution UHPLC-ESI(+)-Q-ToF-MS Data<sup>a,b</sup>**

	tentative identification	retention time (min)	UV $\lambda_{\max}$ (nm)	$[M]^+ / [M + H]^+$ ( $m/z$ )	fragment ions ( $m/z$ )	measured mass	calculated mass	mass error (ppm)	content (mg/g)	identified with
NAAB Extracts										
Hydroxycinnamic Acids										
1	caffeic acid derivatives	7.6	320	579.1472	419.1585, 360.1343, 181.0477	578.1399			3.03 ± 0.16	UV, MS, Q-ToF
2	chlorogenic acid	8.2	326	355.1046	163.0428	354.0973	354.0951	6.21	10.39 ± 0.36	UV, MS, Q-ToF
3	unknown	19.4	318	559.1393	449.1748, 249.2034	558.1320			5.89 ± 0.17	UV, MS, Q-ToF
	total hydroxycinnamic acids								19.30 ± 0.39	
Flavonol Glycosides										
4	que-glu, que-gal	20.1	359	465.1052	303.0469, 249.2035	455.0979	464.0954	5.39	5.31 ± 0.21	UV, MS, Q-ToF
5	que-glucuronide	20.6	355	479.0848	303.0472, 249.2036	478.0775	478.0747	5.86	6.32 ± 0.44	UV, MS, Q-ToF
6	unknown	24.3	360	495.1118	249.2045, 130.1579	494.1045			1.20 ± 0.17	UV, MS, Q-ToF
7	que-ara	26.4	355	435.0923	303.0491, 249.2054	434.0850	434.0849	0.21	0.82 ± 0.07	UV, MS, Q-ToF
8	unknown	29.5	365	381.1310	319.0444, 249.2058	380.1237			1.31 ± 0.06	UV, MS, Q-ToF
	total flavonol glycosides								14.96 ± 0.54	
Anthocyanins										
9	del-3-O-gal	8.5	276, 524	465.1052	303.0518	465.1058	465.1033	5.38	51.40 ± 2.74	UV, MS, Q-ToF
10	del-3-O-glu	8.9	278, 524	465.1050	303.0477	465.1055	465.1033	4.73	41.89 ± 1.57	UV, MS, Q-ToF
11	cya-3-O-gal	9.6	280, 517	449.1088	287.0535	449.1083	449.1083	0	49.10 ± 1.29	UV, MS, Q-ToF
12	del-3-O-ara	9.9	276, 524	435.0926	303.0479	435.0931	435.0927	0.92	53.09 ± 1.87	UV, MS, Q-ToF
13	cya-3-O-glu	10.4	280, 517	449.1075	287.0533	449.1080	449.1083	-0.67	40.68 ± 1.49	UV, MS, Q-ToF
14	pet-3-O-gal	11.1	278, 526	479.1177	317.0640	479.1182	479.1189	-1.46	20.72 ± 1.32	UV, MS, Q-ToF
15	cya-3-O-ara	11.8	280, 517	419.0964	287.0539	419.0969	419.0978	-2.15	37.08 ± 1.02	UV, MS, Q-ToF
16	pet-3-O-glu	12.1	278, 526	479.1182	317.0644	479.1187	479.1189	-0.42	30.57 ± 0.93	UV, MS, Q-ToF
17	peo-3-O-gal	13.4	280, 519	463.1234	301.0699	463.1239	463.1240	0.22	5.57 ± 0.35	UV, MS, Q-ToF
18	pet-3-O-ara	14.2	275, 522	449.1081	317.0648	449.1086	449.1083	0.67	12.32 ± 0.39	UV, MS, Q-ToF
19	peo-3-O-glu	15.2	280, 317	463.1244	301.0703	463.1249	463.1240	-1.94	18.77 ± 0.33	UV, MS, Q-ToF

F

Table 1. continued

	tentative identification	retention time (min)	UV $\lambda_{\max}$ (nm)	$[M]^+/[M + H]^+$ ( $m/z$ )	fragment ions ( $m/z$ )	measured mass	calculated mass	mass error (ppm)	content (mg/g)	identified with
20	mal-3-O-gal	16	278, 527	493.1352	331.0797	493.1357	493.1346	2.23	16.23 ± 0.59	UV, MS, Q-ToF
21	peo-3-O-ara	17.8	280, 520	433.1143	301.0656	433.1148	433.1134	3.23	3.17 ± 0.08	UV, MS, Q-ToF
22	mal-3-O-glu	18.1	278, 526	493.1361	331.0779	493.1366	493.1346	4.06	33.29 ± 0.88	UV, MS, Q-ToF
23	mal-3-O-ara	21.7	280, 522	463.1211	331.0784	463.1216	463.1240	-5.18	10.01 ± 0.36	UV, MS, Q-ToF
	total anthocyanins								423.89 ± 7.02	
					Anthocyanins					
					AAPP Extracts					
1	neochlorogenic acid	5.6	323	355.1011	Hydroxycinnamic Acids 163.0386	354.0938	354.0951	-3.67	1.05 ± 0.05	UV, MS, Q-ToF
2	unknown	6.3	318	531.3165	251.1378	531.3092			3.13 ± 0.13	UV, MS, Q-ToF
3	cryptochlorogenic acid	7.5	326	355.1018	163.0431	354.0945	354.0951	-1.69	17.6 ± 0.45	UV, MS, Q-ToF
4	chlorogenic acid	7.8	329	355.1023	163.0436	354.0950	354.0951	-0.28	93.01 ± 2.91	UV, MS, Q-ToF
5	caffeic acid	8.6	323	181.0484		181.0411	180.0423	-6.66	4.17 ± 0.07	UV, MS, Q-ToF
6	unknown	9.9	312	293.1005	173.0383	293.0932			2.75 ± 0.13	UV, MS, Q-ToF
7	unknown	13.3	327	759.2108	391.0988, 163.0383	758.2035			16.23 ± 1.07	UV, MS, Q-ToF
8	chlorogenic acid derivatives	16.3	315	497.1298	355.0781, 223.0455	496.1223			6.13 ± 0.12	UV, MS, Q-ToF
	total hydroxycinnamic acids								144.07 ± 4.21	
					Anthocyanins					
9	pet-rut-glu	7.7	325, 528	787.2266	444.2220, 317.0635	787.2271	787.2297	-3.30	1.25 ± 0.05	UV, MS, Q-ToF
10	peo-rut-glu	8.6	323, 517	771.2329	474.2581, 301.0686	771.2334	771.2348	-1.81	1.30 ± 0.05	UV, MS, Q-ToF
11	pet-cou-rut-glu; cya-caf-rut-glu	16.9	314, 525	933.2655, 919.2514	639.1936, 317.0658, 372.2685, 287.4533, 303.8841	933.2660; 919.2519	933.2665; 919.2508	-0.53; -1.19	0.92 ± 0.04	UV, MS, Q-ToF
12	pet-caf-rut-glu; del-cou-rut-glu	18.6	279, 531	949.2621, 919.2497	540.8007, 432.2731, 317.0652 303.0491	949.2626; 919.2502	949.2614; 919.2508	1.26, -0.76	12.31 ± 0.26	UV, MS, Q-ToF
13	peo-caf-rut-glu	24.2	281, 524	933.2647	634.2646, 301.1486	933.2652	933.2665	-1.39	1.21 ± 0.02	UV, MS, Q-ToF
14	peo-cou-rut-glu	25.3	300, 520	903.2545	479.1280, 301.0638	903.2550	903.2559	-0.99	9.06 ± 0.08	UV, MS, Q-ToF
15	pet-cou-rut-glu	28.0	279, 532	933.2654	641.1713, 641.1704, 317.0641	933.2659	933.2665	-1.17	160.82 ± 4.39	UV, MS, Q-ToF
16	pet-fer-rut-glu	31.7	280, 532	963.2776	641.1729, 508.5993, 317.0658	963.2781	963.2770	1.14	7.30 ± 0.32	UV, MS, Q-ToF

Table 1. continued

tentative identification	retention time (min)	UV $\lambda_{\max}$ (nm)	$[M]^+/[M + H]^+$ (m/z)	fragment ions (m/z)	measured mass	calculated mass	mass error (ppm)	content (mg/g)	identified with
				Anthocyanins					
17	33.8	280, 507	887.2605	638.3073, 456.2497	887.2610	887.2610	0	0.96 ± 0.03	UV, MS, Q-ToF, Lit1
18	36.4	307, 522	917.2693	463.1213, 301.0685	917.2716	917.2716	-1.96	40.30 ± 2.23	UV, MS, Q-ToF
19	38.6	280, 529	947.2795	655.1854, 500.5989, 331.0791	947.2800	947.2821	-2.22	8.70 ± 0.45	UV, MS, Q-ToF
20	40.2	320, 534	947.2806	625.1757, 500.5997	947.2811	947.2821	-1.06	2.81 ± 0.1	UV, MS, Q-ToF, Lit1
21	41.5	305, 530	977.2919	622.4004, 490.2943, 331.0810	977.2924	977.2927	-0.31	0.76 ± 0.02	UV, MS, Q-ToF
22	43.3	300, 530	771.2138	446.7790, 446.7790, 367.1968	771.2143	771.2136	0.91	1.04 ± 0.09	UV, MS, Q-ToF
total anthocyanins								248.74 ± 7.14	

<sup>a</sup>The positive ions  $M^+$  for anthocyanins and  $[M + H]^+$  for hydroxycinnamic acids and flavonol glycosides. Numbering of the peaks refers to Figure 1. <sup>b</sup>Abbreviations: que, quercetin; cya, cyanidin; del, delphinidin; mal, malvidin; pel, pelargonidin; peo, peonidin; pet, petunidin; caf, caffeic acid; cou, coumaric acid; fer, ferulic acid; glu, glucoside; ara, arabinose; rut, rutinose; and gal, galactose. Amounts are given as mg per g extracts ± standard deviation,  $n = 3$ .

metabolism. However, most of the metabolites showed a similar trend in the Con and ND groups compared to that in the M group, indicating that the impact of differences in feeds was low.

**Impact of Nonacylated and Acylated Anthocyanin-Rich Extracts on the Plasma Metabolomic Profile of ZDF Rats.** To further explore the detailed alterations in plasma metabolites as impacted by the anthocyanin extracts, univariate analysis for discriminating metabolites among the groups was performed (Figure 4) and their fold change value compared to that in the M groups is shown in Table S4. Treatment with the anthocyanin extracts from bilberries and purple potatoes (H-NAAB, H-AAPP, L-NAAB, and L-AAPP) resulted in alteration in the levels of various metabolites as compared to that in the M group, suggesting possible improvement of diabetic state. Lower levels of GLU were observed in the L-NAAB, H-NAAB, L-AAPP, and H-AAPP groups ( $p < 0.001$ ,  $p < 0.01$ ,  $p > 0.05$ , and  $p > 0.05$ , compared with that in the M group), confirming the findings of the biochemical assays (Figure 4A). Resonances from lipids and unsaturated lipids were also decreased by all anthocyanin treatment groups (L-NAAB:  $p > 0.05$ ,  $p < 0.05$ ; H-NAAB:  $p < 0.01$ ,  $p < 0.01$ ; L-AAPP:  $p < 0.001$ ,  $p < 0.01$ ; H-AAPP:  $p < 0.05$ ,  $p > 0.05$ ) (Figure 4B). There was an overall decrease of BCAAs in all anthocyanin-treated groups, especially in the groups fed with AAPP (Figure 4C). In addition to common changes in metabolites by the anthocyanin extracts mentioned above, the L-AAPP group showed a decreased level of lactate ( $p < 0.01$ ) and pyruvate ( $p < 0.01$ ) (Figure 4A,D). The H-AAPP group shared the same decreasing trend in lactate ( $p < 0.05$ ) and pyruvate ( $p > 0.05$ ). Both L-AAPP and H-AAPP significantly decreased glycerol ( $p < 0.01$ ,  $p < 0.01$ ), the glutamate level ( $p < 0.01$ ,  $p < 0.01$ ), the glutamine/glutamate ratio ( $p < 0.05$ ,  $p < 0.05$ ), and serine ( $p < 0.01$ ,  $p < 0.05$ ) (Figure 4D–F). A decreased choline level was seen in both the L-AAPP and H-AAPP groups ( $p < 0.05$ ,  $p < 0.01$ ).

**Metabolic Pathway Analysis and Correlation Analysis.** Metabolic pathway analysis generated with the MetaboAnalyst tool is shown in Figure 5. Starch and sucrose metabolism were the most significantly altered pathways with high impact values when comparing the Con, ND, L-NAAB, or H-NAAB groups to the M group (Figure 5A–D) because of the differences in plasma GLU levels. Statistically significant differences were also detected in glutamine and glutamate metabolism, pyruvate metabolism, alanine, aspartate and glutamate metabolism, and glycine, serine, and threonine metabolism between the M and Con/ND groups. AAPP influenced many pathways, including glutamine and glutamate metabolism, phenylalanine, tyrosine and tryptophan biosynthesis, histidine metabolism, phenylalanine metabolism, and pyruvate metabolism. In contrast to AAPP, NAAB from bilberries did not show significant impact on these pathways. This is in agreement with the findings discussed in previous sections, suggesting that AAPP affected more metabolites than NAAB in type 2 diabetes in ZDF rats. Correlation analysis was made to investigate the correlation between plasma metabolites and biochemical parameters. The heatmap was designed using Pearson's  $r$  analysis (Figure S6). The main finding from the correlation plot was that the glutamine/glutamate ratio, glutamine, AST, histidine, 3-hydroxybutyrate, and acetoacetate were negatively correlated with glutamate, glycerol, the lipid profile (lipid, unsaturated lipid, and TG), and glycolysis metabolites (GLU, lactate, pyruvate, citrate, and alanine).

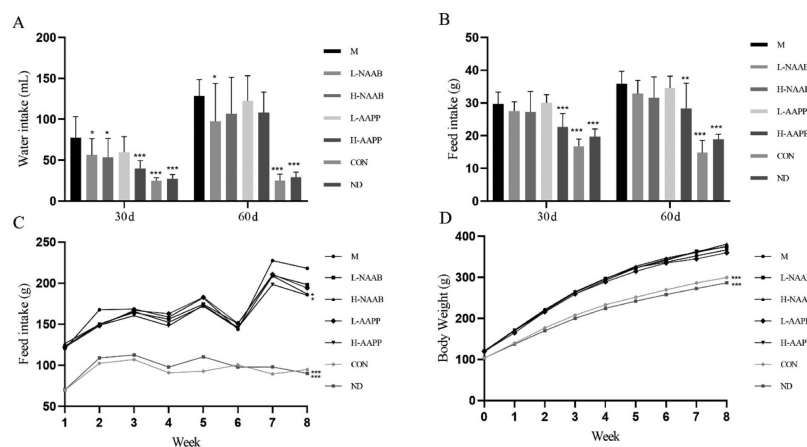


**Figure 2.** Effect of anthocyanins extracted from bilberries and purple potatoes on water (A) and feed (B) intake on the 30th day and 60th day of intervention, weekly feed intake (C), and weekly body weight (D) in lean Zucker rats and ZDF rats fed with the different experimental diets. Experimental groups: M, ZDF rats given high-fat diet; L-NAAB, ZDF rats fed with high-fat diet supplemented with low-dose nonacylated anthocyanins from bilberries; H-NAAB, ZDF rats fed with high-fat diet supplemented with high-dose nonacylated anthocyanins from bilberries; L-AAPP, ZDF rats fed with high-fat diet supplemented with low-dose acylated anthocyanins from purple potatoes; H-AAPP, ZDF rats fed with high-fat diet supplemented with high-dose acylated anthocyanins from purple potatoes; Con, lean Zucker rats given high-fat diet; and ND, lean Zucker rats given normal diet. \* $p < 0.05$ , \*\* $p < 0.01$ , and \*\*\* $p < 0.001$  as compared with the M group.

**Table 2.** Changes of Fasting Plasma Parameters in Lean Zucker Rats and ZDF Rats Fed with Different Experimental Diets<sup>a</sup>

	M	L-NAAB	H-NAAB	L-AAPP	H-AAPP	Con	ND
ALT (U/L)	137.7 ± 22.8	190.1 ± 24.3	196.4 ± 52.7	181.8 ± 33.4	217.2 ± 53.3	164.6 ± 36.9	193.6 ± 54.6
TP (g/L)	63.2 ± 5.3	65.4 ± 6.3	64.2 ± 3.8	60.5 ± 3.7	63.6 ± 6.7	52.8 ± 1.1**	53.2 ± 2.4**
ALB (g/L)	28.5 ± 1.8	30.2 ± 1.7	30.2 ± 2.1	28.1 ± 1.6	28.1 ± 1.6	28.7 ± 1.5	29.1 ± 0.7
AST (U/L)	335.6 ± 136.9	485.4 ± 79.0	462.3 ± 72.2	454.0 ± 99.6	584.6 ± 139.6	869.3 ± 133.4***	1016.2 ± 229.6**
BUN (mmol/L)	7.3 ± 1.4	7.8 ± 2.3	7.6 ± 1.3	7.2 ± 0.5	7.0 ± 1.4	5.1 ± 0.9**	5.4 ± 0.5**
TG (mmol/L)	8.77 ± 2.75	8.61 ± 4.84	7.55 ± 2.63	6.93 ± 2.62	6.61 ± 2.22	1.27 ± 0.35**	1.05 ± 0.16**
Insulin (mU/L)	33.67 ± 14.75	29.56 ± 11.47	38.51 ± 13.66	39.91 ± 6.10	42.50 ± 10.23	42.44 ± 24.51	35.44 ± 13.45
GLU (mmol/L)	23.0 ± 1.9	14.5 ± 3.3***	16.4 ± 4.3**	20.8 ± 7.8	20.4 ± 6.2	10.9 ± 1.3***	8.5 ± 1.0***

<sup>a</sup>ALT, alanine transaminase; TP, total protein; ALB, albumin; AST, aspartate transaminase; BUN, blood urea nitrogen; and TG, triacylglycerols; data represent the means ± SD,  $n = 8$ . Experimental groups: M, Zucker diabetic fatty (ZDF) rats given high-fat diet; L-NAAB, ZDF rats fed with high-fat diet supplemented with low-dose nonacylated anthocyanins from bilberries; H-NAAB, ZDF rats fed with high-fat diet supplemented with high-dose nonacylated anthocyanins from bilberries; L-AAPP, ZDF rats fed with high-fat diet supplemented with low-dose acylated anthocyanins from purple potatoes; H-AAPP, ZDF rats fed with high-fat diet supplemented with high-dose acylated anthocyanins from purple potatoes; Con, lean Zucker rats given high-fat diet; and ND, lean Zucker rats given normal diet. \* $p < 0.05$ , \*\* $p < 0.01$ , and \*\*\* $p < 0.001$  as compared with the M group; # $p < 0.05$  as compared with the ND group.

Importantly, several metabolites were correlated with the improvements in the glycemia status. The GLU level was negatively correlated with histidine (Pearson correlation coefficient  $r = -0.74$ ,  $p < 0.001$ ), glycine ( $r = -0.45$ ,  $p < 0.01$ ), glutamine ( $r = -0.64$ ,  $p < 0.0001$ ), glutamine/glutamate ratio ( $r = -0.34$ ,  $p < 0.05$ ), and tyrosine ( $r = -0.43$ ,  $p < 0.01$ ). On the other hand, there was a positive correlation between plasma GLU level and lipid ( $r = 0.74$ ,  $p < 0.001$ ), unsaturated lipid ( $r = 0.73$ ,  $p < 0.001$ ), lactate ( $r = 0.36$ ,  $p < 0.05$ ), pyruvate ( $r = 0.56$ ,  $p < 0.001$ ), citrate ( $r = 0.44$ ,  $p < 0.01$ ), valine ( $r = 0.45$ ,  $p < 0.01$ ), and isoleucine ( $r = 0.50$ ,  $p < 0.001$ ).

## DISCUSSION

As reviewed by Belwal *et al.*,<sup>23</sup> the mechanisms *via* which anthocyanins affect insulin resistance and type 2 diabetes include at least activating the AMPK and lipolytic enzymes, upregulating glucose transporter 4 (GLUT4) translocations, decreasing the serine phosphorylation of insulin receptor substrate 1 and sterol regulatory element-binding protein 1 (SREBP-1), and inhibiting fatty acid and triacylglycerol synthesis. Previously, a <sup>1</sup>H NMR metabolomic study showed

that adding quercetin to the feed affected the Krebs cycle as well as amino acid and carbohydrate metabolism in healthy Sprague Dawley rats.<sup>24</sup> However, the effect of anthocyanin extracts on the plasma metabolic profile of the healthy or type 2 diabetic state has not been studied before either in humans or in animals. Therefore, the current study is the first report on the effects of anthocyanins on the plasma metabolic profile of the diabetic state. To the best of our knowledge, it is also the first study comparing the effect of nonacylated anthocyanins with their acylated counterparts in their metabolic impact on type 2 diabetes.

Alterations in the feed and water intake, body weight, GLU level, and lipid profile were evident between the diabetic rats fed with high-fat diet without anthocyanins (M group) in comparison with the two groups of lean Zucker rats on high-fat diet (Con) or normal feed (ND), indicating the significant impact of leptin gene deficiency and the successful establishment of the diabetic model in the model group. In this study, the ALT level, an indicator of liver function, did not differ between the ZDF rats and the lean Zucker rats, which was in agreement with previous findings.<sup>25</sup> On the other hand, the



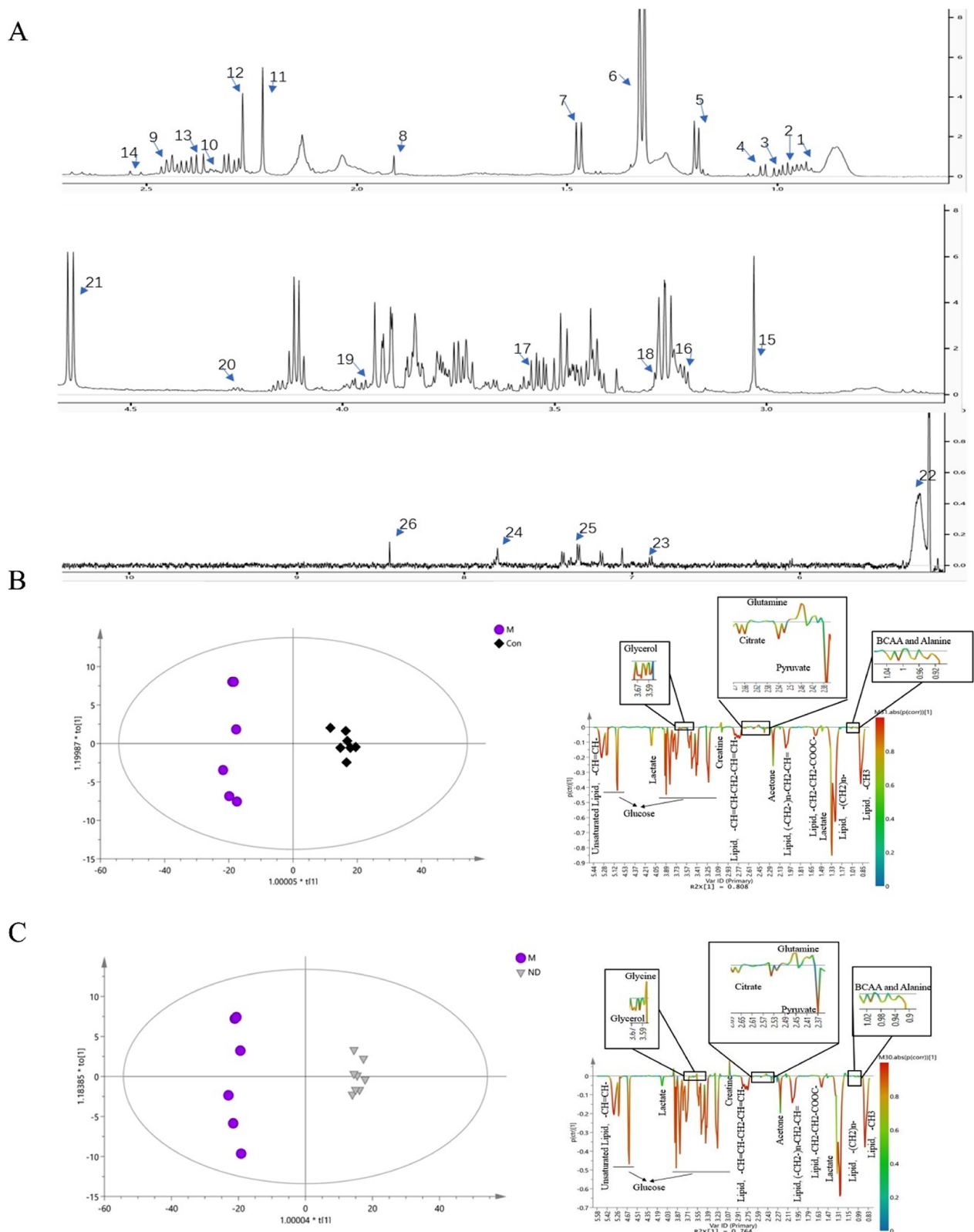


**Figure 3.** 600 MHz 1D CPMG  $^1\text{H}$  NMR spectrum of plasma labeled with identified metabolites (A): (1) lipids,  $-\text{CH}_3$ , (2) isoleucine, (3) valine, (4) leucine, (5) 3-hydroxybutyrate, (6) lactate, (7) alanine, (8) glutamine, (9) glutamate, (10) acetone, (11) acetoacetate, (13) pyruvate, (14) citrate, (15) creatine/creatinine, (16) choline, (17) glycine, (18) glycerol, (19) serine, (20) threonine, (21) GLU, (22) unsaturated lipid,  $-\text{CH}=\text{CH}-$ , (23) tyrosine, (24) histidine, (25) phenylalanine, and (26) formate. Details on the assignment of peaks refer to Table S3. OPLS-DA and the loading  $S$  line plot of the Con group vs M group and ND group vs M group (B,C) based on  $^1\text{H}$  NMR spectra of plasma. The color bar corresponds to the value of correlation coefficients, and the red signal indicates more significant contribution to the class separation than a green one. The negative side of the loading plot constituted metabolites increased in the M group. Experimental groups: Con, lean Zucker rats given high-fat diet; M, ZDF rats given high-fat diet; and ND, lean Zucker rats given normal diet.

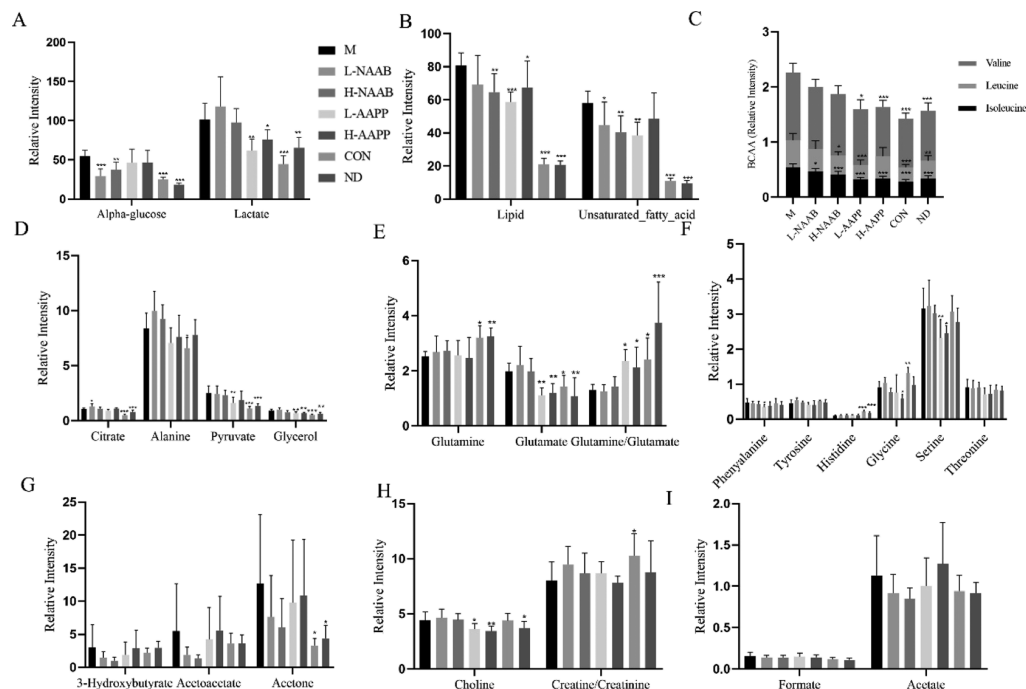


**Figure 4.** Effect of supplement of L-NAAB, H-NAAB, L-AAPP, and H-AAPP on plasma metabolites in ZDF rats. (A)  $\alpha$ -GLU and lactate. (B) Lipid and unsaturated lipid. (C) BCAAs, branched-chain amino acids (valine, leucine, and isoleucine). (D) Citrate, alanine, pyruvate, and glycerol. (E) Glutamine, glutamate, and glutamine/glutamate ratio. (F) Phenylalanine, tyrosine, histidine, glycine, serine, and threonine. (G) Ketone bodies. (H) Choline and creatine/creatinine. (I) Formate and acetate. Experimental groups: M, ZDF rats given high-fat diet; L-NAAB, ZDF rats fed on high-fat diet supplemented with low-dose nonacylated anthocyanins from bilberries; H-NAAB, ZDF rats fed on high-fat diet supplemented with high-dose nonacylated anthocyanins from bilberries; L-AAPP, ZDF rats fed on high-fat diet supplemented with low-dose acylated anthocyanins from purple potatoes; H-AAPP, ZDF rats fed on high-fat diet supplemented with high-dose acylated anthocyanins from purple potatoes; Con, lean Zucker rats given high-fat diet; and ND, lean Zucker rats given normal diet. \* $p < 0.05$ , \*\* $p < 0.01$ , and \*\*\* $p < 0.001$  as compared with the M group. Bar labels are the same for all subfigures, except subfigure (C).

plasma levels of AST, which is involved in the amino acid metabolism, were remarkably higher in lean Zucker rats (Con and ND groups) as compared to the levels in all the groups of diabetic rats including the M group and all the groups treated with the anthocyanin extracts. Any alteration in AST level in the liver, heart, muscle, kidney, or blood cells may have contributed to the circulating level of AST in plasma. The lowered level of AST in the ZDF rats could have also resulted from the deficiency in the *leptin* receptor gene. We did not see higher levels of plasma insulin in the groups of ZDF rats than the normal rats in the ND group, indicating possible decline of the function of  $\beta$ -cells in ZDF rats after the age of 10 weeks.<sup>26</sup>

As a successful manifestation of the type 2 diabetes model, a higher level of plasma fasting GLU as well as elevation in lipid accumulation was seen in the ZDF rats fed with high-fat feed (M) compared to the lean Zucker rats (Con and ND) as seen both with the NMR metabolomic study (Figure 4) and the biochemical assays. Feeding with anthocyanins, especially with nonacylated anthocyanins reduced the plasma GLU levels compared to the M group without anthocyanin addition. Our previous studies with both purple potatoes and anthocyanin extract from purple potatoes of *S. tuberosum* L. 'Synkeä Sakari' have indicated positive effects of potato anthocyanins on postprandial levels of plasma GLU and insulin in healthy men.<sup>19,22</sup> In the present study, the levels of total lipids and unsaturated lipids were decreased in all anthocyanin-treated groups, independent of weight loss, which might have resulted from an increase in lipid catabolism and/or a decrease in lipogenesis.

Development of type 2 diabetes brings about a compensatory increase in glycolysis.<sup>27</sup> High plasma levels of lactate, citrate, alanine, and pyruvate in the M group compared to those in the ND/Con groups indicated an overall high level of glycolysis. An increased lactate level is caused by aberrant pyruvate metabolism, in which pyruvate is converted to lactate instead of being converted to acetyl-CoA because of the inactivation of pyruvate dehydrogenase and increased NADH/NAD<sup>+</sup> ratios.<sup>28</sup> Moreover, increased lactate can result from hypoxia in the skeletal muscle and adipose tissue caused by the decrease in the lactate transporter monocarboxylate transport protein 1 and obesity, respectively.<sup>29</sup> Oxidative stress in type 2 diabetes increases the activities of lactate dehydrogenase and thus induces the increment of the lactate level.<sup>30</sup> Anthocyanins have shown strong antioxidative activities.<sup>31</sup> In our study, the groups fed with L-AAPP showed a significant decrease in lactate, citrate, and pyruvate compared with the model group (M), indicating improved glycolysis and/or oxidative stress. Moreover, serine can be converted to glycine and continue to donate carbon of its side chain to form folate.<sup>32</sup> In our experiment, acylated anthocyanins from potatoes at both doses decreased the levels of lactate, serine, and glycine, which might have been associated with improvement in the oxidative status in the diabetic rats. AAPP contained a higher content of chlorogenic acid ( $93.01 \pm 2.91$  mg/g) than NAAB ( $10.39 \pm 0.36$  mg/g), which could also have contributed to the reduction in serum lactate and pyruvate levels.<sup>33</sup> Glycerol is an important intermediate in lipid synthesis and lipolysis in the liver as well as a substrate for gluconeogenesis.<sup>34</sup> AAPP decreased the plasma glycerol level, which might be linked with

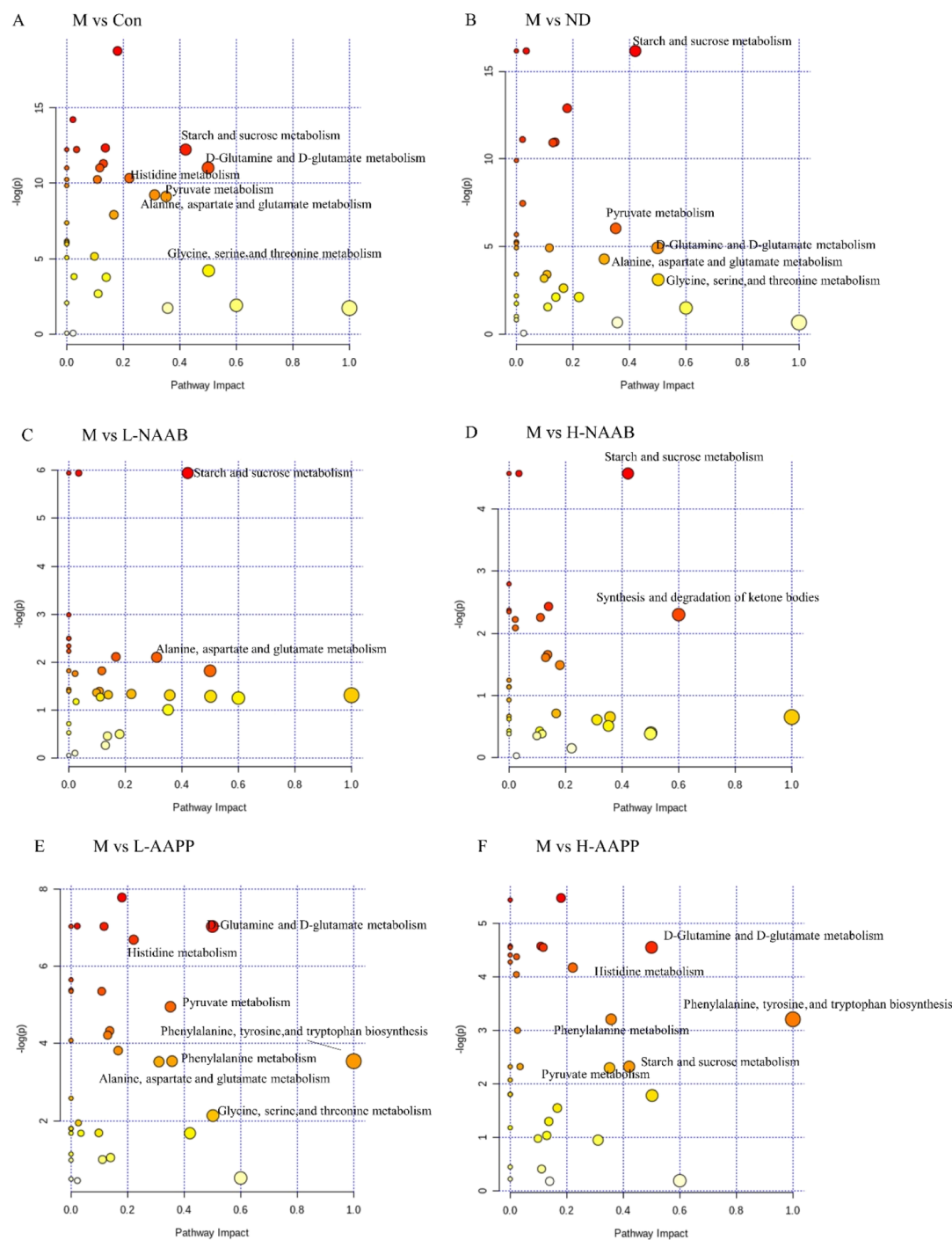


**Figure 5.** Metabolic pathway analysis generated with the MetaboAnalyst software package based on metabolites identified from plasma NMR spectra, showing altered pathways between M and Con (A), M and ND (B), M and L-NAAB (C), M and H-NAAB (D), M and L-AAPP (E), and M and H-AAPP (F). The  $p$ -values in the Y-axis are generated from the pathway enrichment analysis, and the X-axis presents the pathway impact values from pathway topology analysis. The node color indicates the  $p$ -value from the pathway enrichment analysis (more reddish color indicates more significant changes in the pathway), whereas the node size reflects the pathway impact score. Pathways with small  $p$ -values and large pathway impact scores are considered as highly influential. Experimental groups: M, ZDF rats given high-fat diet; L-NAAB, ZDF rats fed on high-fat diet supplemented with low-dose nonacylated anthocyanins from bilberries; H-NAAB, ZDF rats fed with high-fat diet supplemented with high-dose nonacylated anthocyanins from bilberries; L-AAPP, ZDF rats fed with high-fat diet supplemented with low-dose acylated anthocyanins from purple potatoes; H-AAPP, ZDF rats fed on high-fat diet supplemented with high-dose acylated anthocyanins from purple potatoes; Con, lean Zucker rats given high-fat diet; and ND, lean Zucker rats given normal diet.

a decreased level of lipid metabolism and a lower level of gluconeogenesis.

Levels of amino acids regulate protein synthesis, gluconeogenesis, and syntheses of hormones, urea, and low-molecular-

weight nitrogenous substances.<sup>32</sup> Increased levels of circulating BCAAs, as observed in the model group of ZDF rats compared with the groups of lean rats, are associated with insulin resistance and dysregulation of metabolism of sugars and

lipids.<sup>35</sup> The plasma levels of BCAAs are controlled by the activities of branched-chain ketoacid dehydrogenase kinase (BDK) and mitochondrial phosphatase 2C (PP2Cm), commonly known as the kinase and phosphatase pair. In obesity and type 2 diabetes, high activity of PP2Cm leads to hyperphosphorylation of BDK by PP2Cm, resulting in suppression of BDK activity and increased levels of BCAAs. Also, a high level of PP2Cm activity can activate adenosine 5'-triphosphate citrate lyase and upregulate the conversion of citrate to acetyl CoA and malonyl CoA, which serve as the immediate substrates for lipogenesis and inhibit fatty acid oxidation *via* allosteric inhibition of carnitine palmitoyltransferase-1.<sup>36</sup> Compared with the diabetic group fed with high-fat diet without anthocyanins (group M), there was an overall decreasing trend in BCAAs and lipids in all the groups fed with the anthocyanin extracts; this could be indicative of improvement in insulin sensitivity and reduction in lipogenesis. Comparing the two anthocyanin extracts, the potato anthocyanin extract showed stronger impact on BCAA than the bilberry anthocyanin extract.

Glucose-6-phosphatase (G6Pase) encoded by the *G6PC* gene hydrolyzes glucose 6-phosphate releasing GLU into the circulation.<sup>37</sup> Decreased hepatic *G6PC* gene expression was seen at the transcription level in all anthocyanin treatment groups, and especially, the decrease was statistically significant in the groups fed with acylated anthocyanins (Figure S1). Glycerol as a major gluconeogenic substrate may also induce the expression of G6Pase catalyzing the terminal enzymatic step in gluconeogenesis.<sup>38</sup> In the current study, both the circulating level of glycerol and mRNA of the *G6PC* gene were decreased in the groups fed with the potato anthocyanin extract. Furthermore, chlorogenic acid present in the extract may have had an inhibiting effect on the G6Pase system.<sup>39</sup> These findings suggest the impact of the potato extract on GLU homeostasis by regulating glycogenolysis and gluconeogenesis. *TBC1D1* regulates the translocation of GLUT4 from intracellular vesicles to the surface of cell membranes in response to insulin stimulation, playing an important role in energy homeostasis.<sup>40</sup> The expression and regulating role of *TBC1D1* are tissue-specific.<sup>41</sup> *TBC1D1* deficiency enhanced the suppression of hepatic GLU production during euglycemic hyperinsulinemic clamping in 4 h fasting mice, indicating improved insulin sensitivity compared to the wild type.<sup>41</sup> The *TBC1D1* knock-in mice developed obesity and displayed characteristics of metabolic syndromes because of an increase in the expression of insulin-like growth factor 1 in hepatocytes and activation of the expression of lipogenic genes.<sup>42</sup> In this study, feeding with H-AAPP significantly decreased hepatic mRNA levels of the *TBC1D1* gene in ZDF rats (Figure S1), indicating possible regulation of gene expression of *TBC1D1*. In addition, anthocyanins could also modulate other genes associated with energy metabolism: feeding anthocyanins from purple corn decreased hepatic fatty acid synthase, acyl-CoA synthase1, glycerol-3-phosphate acyltransferase, and SREBP-1 in high-fat-diet-induced insulin resistance mice;<sup>43</sup> feeding with the mulberry anthocyanin extract could increase hepatic peroxisome proliferator-activated receptor- $\gamma$  coactivator-1 $\alpha$ , AMP-activated protein kinase  $\alpha$ , and SREBP-1c in *db/db* mice.<sup>44</sup>

A clinical study has found a significant positive correlation between the plasma level of glutamate and insulin resistance,<sup>45</sup> and an increase in glutamine/glutamate ratio predicted a reduced risk for developing diabetes.<sup>45,46</sup> Increased glutamine

and decreased glutamate might be associated with increased levels of glucagon-like peptide-1, enhancement of the vesicle trafficking of GLUT4, and improvement in insulin secretion and insulin sensitivity.<sup>47,48</sup> In our current study, the M group had a significantly lower glutamine/glutamate ratio compared to the groups Con and ND, and the treatment with the purple potato anthocyanin extract rich in acylated anthocyanins significantly increased the glutamine/glutamate ratio, indicating improved insulin secretion and/or insulin sensitivity. The nonacylated bilberry anthocyanin extract did not show clear impact on the glutamine/glutamate ratio. Therefore, the mechanism for reducing the GLU level in plasma observed of the bilberry anthocyanin extract was likely not related to glutamine/glutamate ratio. Acetone was significantly higher in the M group, whereas other ketone bodies (acetoacetate and 3-hydroxybutyrate) remain unchanged, indicating a high clearance rate for these two ketone bodies in ZDF rats.

The metabolic pathway analysis illustrated different metabolic impacts on ZDF rats between the potato extract rich in acylated anthocyanins and the bilberry extract rich in nonacylated anthocyanins. The bilberry extract influenced mainly on carbohydrate (starch) metabolisms, whereas the potato extract altered the pathways of a wide range of amino acid metabolisms and carbohydrate metabolisms.

In addition to the difference in different compositions and acylation status of the anthocyanins between the two extracts, phenolic acids, especially the higher content of chlorogenic acid in the potato extract, could have contributed to the different metabolic impacts observed among the groups treated with these extracts.<sup>33</sup>

In conclusion, ZDF rats showed alteration in a number of plasma metabolites of the key pathways related to energy metabolism and insulin sensitivity. Feeding with anthocyanin extracts ameliorated many of these changes and reverted the metabolic profile toward those of the lean rats. NAAB reduced the plasma GLU levels of obese diabetic ZDF rats. Both the bilberry extract rich in anthocyanins and AAPP reduced the levels of BCAAs and lipids, suggesting improved insulin sensitivity and decreased lipogenesis. Moreover, AAPP and NAAB showed different impacts on the metabolic profiles of ZDF rats. AAPP reversed more of the metabolites to the normal state, and the glutamine/glutamate ratio, glycerol, and metabolites involved in glycolysis were modulated by AAPP, which might be associated with improved insulin sensitivity, gluconeogenesis, glycolysis, and/or oxidative status. Metabolic pathway analysis further revealed clear difference in a number of metabolism pathways between the ZDF rats and lean Zucker rats as well as the different metabolic impacts of acylated and nonacylated anthocyanins on ZDF rats. The hepatic *TBC1D1* and *G6PC* mRNA levels were decreased by AAPP, indicating that AAPP might have modulated gluconeogenesis and lipogenesis by regulating the expression of these genes. To the best of our knowledge, this is the first time that the antidiabetic effects of anthocyanins were investigated by metabolomic profiling. The different effects observed of acylated and nonacylated anthocyanins deserve further investigation. Purple-, blue-, and red-colored potatoes represent a unique agricultural produce, providing an affordable source of acylated anthocyanins as health-promoting food ingredients to a large fraction of global population.



## ■ ASSOCIATED CONTENT

### Supporting Information

The Supporting Information is available free of charge at <https://pubs.acs.org/doi/10.1021/acs.jafc.0c04125>.

Composition of the diets, bins for quantification of metabolites, <sup>1</sup>H chemical shift assignments of the metabolites, fold change of the metabolites compared to the M group, hepatic gene expression of *G6PC* and *TBC1D1*, 2D NMR spectrum for plasma, permutation tests of Con group versus M group and ND group versus M group, and correlation plot (PDF)

## ■ AUTHOR INFORMATION

### Corresponding Authors

**Baoru Yang** – Food Chemistry and Food Development, Department of Biochemistry, University of Turku, Turku FI-20014, Finland; [orcid.org/0000-0001-5561-514X](https://orcid.org/0000-0001-5561-514X); Phone: +358 452737988; Email: [baoru.yang@utu.fi](mailto:baoru.yang@utu.fi)

**Yumei Zhang** – Department of Nutrition and Food Hygiene, School of Public Health, Peking University, Beijing 100191, China; Phone: +8613426134251; Email: [zhangyumei@bjmu.edu.cn](mailto:zhangyumei@bjmu.edu.cn)

### Authors

**Kang Chen** – Food Chemistry and Food Development, Department of Biochemistry, University of Turku, Turku FI-20014, Finland; [orcid.org/0000-0002-5791-9523](https://orcid.org/0000-0002-5791-9523)

**Xuetao Wei** – Beijing Key Laboratory of Toxicological Research and Risk Assessment for Food Safety, School of Public Health, Peking University, Beijing 100191, China

**Jian Zhang** – Department of Nutrition and Food Hygiene, School of Public Health, Peking University, Beijing 100191, China

**Raghunath Pariyani** – Food Chemistry and Food Development, Department of Biochemistry, University of Turku, Turku FI-20014, Finland

**Johanna Jokioja** – Food Chemistry and Food Development, Department of Biochemistry, University of Turku, Turku FI-20014, Finland

**Maaria Kortensniemi** – Food Chemistry and Food Development, Department of Biochemistry, University of Turku, Turku FI-20014, Finland

**Kaisa M. Linderborg** – Food Chemistry and Food Development, Department of Biochemistry, University of Turku, Turku FI-20014, Finland

**Jari Heinonen** – School of Engineering Science, Lappeenranta University of Technology, Lappeenranta FI-53850, Finland; [orcid.org/0000-0002-1308-4755](https://orcid.org/0000-0002-1308-4755)

**Tuomo Sainio** – School of Engineering Science, Lappeenranta University of Technology, Lappeenranta FI-53850, Finland

Complete contact information is available at: <https://pubs.acs.org/doi/10.1021/acs.jafc.0c04125>

### Author Contributions

<sup>†</sup>K.C. and X.W. contributed equally.

### Notes

The authors declare no competing financial interest.

## ■ ACKNOWLEDGMENTS

The present work was supported by the Competitive funding to strengthen universities' research profiles from the Academy of Finland (decision no. 318894), by ERVA of the City of

Turku (award no. 604123), by the key projects of Beijing Science and Technology (decision no. D171100008017002), and by a personal grant from the China Scholarship Council (grant no. 201706790015). The authors wish to thank the members of the Instrument Center of the University of Turku for their helpful training of using NMR.

## ■ ABBREVIATIONS

AAPP, acylated anthocyanin extract from purple potatoes; ALT, alanine transaminase; AST, aspartate transaminase; BCAAs, branched-chain amino acids; CPMG, Carr–Purcell–Meiboom–Gill; *G6Pase*, glucose-6-phosphatase; *G6PC*, glucose-6-phosphatase catalytic subunit gene; GLUT4, glucose transporter 4; NAAB, nonacylated anthocyanin extract from bilberries; *TBC1D1*, *TBC1* domain family member 1; ZDF rat, Zucker diabetic fatty rat

## ■ REFERENCES

- (1) Urpi-Sarda, M.; Almanza-Aguilera, E.; Tulipani, S.; Tinahones, F. J.; Salas-Salvadó, J.; Andres-Lacueva, C. Metabolomics for Biomarkers of Type 2 Diabetes Mellitus: Advances and Nutritional Intervention Trends. *Curr. Cardiovasc. Risk Rep.* **2015**, *9*, 12.
- (2) Ali Asgar, M. Anti-Diabetic Potential of Phenolic Compounds: A Review. *Int. J. Food Prop.* **2013**, *16*, 91–103.
- (3) Neyrinck, A. M.; Van Hée, V. F.; Bindels, L. B.; De Backer, F.; Cani, P. D.; Delzenne, N. M. Polyphenol-Rich Extract of Pomegranate Peel Alleviates Tissue Inflammation and Hypercholesterolaemia in High-Fat Diet-Induced Obese Mice: Potential Implication of the Gut Microbiota. *Br. J. Nutr.* **2013**, *109*, 802–809.
- (4) Kay, C. D. Aspects of Anthocyanin Absorption, Metabolism and Pharmacokinetics in Humans. *Nutr. Res. Rev.* **2006**, *19*, 137–146.
- (5) Faria, A.; Fernandes, I.; Norberto, S.; Mateus, N.; Calhau, C. Interplay between Anthocyanins and Gut Microbiota. *J. Agric. Food Chem.* **2014**, *62*, 6898–6902.
- (6) He, J.; Giusti, M. M. Anthocyanins: Natural Colorants with Health-Promoting Properties. *Annu. Rev. Food Sci. Technol.* **2010**, *1*, 163–187.
- (7) Bakowska-Barczak, A. Acylated Anthocyanins as Stable, Natural Food Colorants—a Review. *Pol. J. Food Nutr. Sci.* **2005**, *14*, 107–116.
- (8) D'Auria, J. C. Acyltransferases in Plants: A Good Time to Be BAH. *Curr. Opin. Plant Biol.* **2006**, *9*, 331–340.
- (9) Xu, J.; Su, X.; Lim, S.; Griffin, J.; Carey, E.; Katz, B.; Tomich, J.; Smith, J. S.; Wang, W. Characterisation and Stability of Anthocyanins in Purple-Fleshed Sweet Potato P40. *Food Chem.* **2015**, *186*, 90–96.
- (10) Moriya, C.; Hosoya, T.; Agawa, S.; Sugiyama, Y.; Kozono, I.; Shin-ya, K.; Terahara, N.; Kumazawa, S. New Acylated Anthocyanins from Purple Yam and Their Antioxidant Activity. *Biosci., Biotechnol., Biochem.* **2015**, *79*, 1484–1492.
- (11) Matsui, T.; Ueda, T.; Oki, T.; Sugita, K.; Terahara, N.; Matsumoto, K.  $\alpha$ -Glucosidase Inhibitory Action of Natural Acylated Anthocyanins. 2.  $\alpha$ -Glucosidase Inhibition by Isolated Acylated Anthocyanins. *J. Agric. Food Chem.* **2001**, *49*, 1952–1956.
- (12) Oliveira, H.; Perez-Gregório, R.; de Freitas, V.; Mateus, N.; Fernandes, I. Comparison of the in Vitro Gastrointestinal Bioavailability of Acylated and Non-Acylated Anthocyanins: Purple-Fleshed Sweet Potato vs Red Wine. *Food Chem.* **2019**, *276*, 410–418.
- (13) Kurilich, A. C.; Clevidence, B. A.; Britz, S. J.; Simon, P. W.; Novotny, J. A. Plasma and Urine Responses Are Lower for Acylated vs Nonacylated Anthocyanins from Raw and Cooked Purple Carrots. *J. Agric. Food Chem.* **2005**, *53*, 6537–6542.
- (14) Charron, C. S.; Kurilich, A. C.; Clevidence, B. A.; Simon, P. W.; Harrison, D. J.; Britz, S. J.; Baer, D. J.; Novotny, J. A. Bioavailability of Anthocyanins from Purple Carrot Juice: Effects of Acylation and Plant Matrix. *J. Agric. Food Chem.* **2009**, *57*, 1226–1230.
- (15) Zamora-Ros, R.; Knaze, V.; Luján-Barroso, L.; Slimani, N.; Romieu, I.; Touillaud, M.; Kaaks, R.; Teucher, B.; Mattiello, A.;

- Grióni, S.; Crowe, F.; Boeing, H.; Förster, J.; Quirós, J. R.; Molina, E.; Huerta, J. M.; Engeset, D.; Skeie, G.; Trichopoulou, A.; Dilis, V.; Tsiotas, K.; Peeters, P. H. M.; Khaw, K.-T.; Wareham, N.; Bueno-De-Mesquita, B.; Ocké, M. C.; Olsen, A.; Tjønneland, A.; Tumino, R.; Johansson, G.; Johansson, I.; Ardanaz, E.; Sacerdote, C.; Sonestedt, E.; Ericson, U.; Clavel-Chapelon, F.; Boutron-Ruault, M.-C.; Fagherazzi, G.; Salvini, S.; Amiano, P.; Riboli, E.; González, C. A. Estimation of the Intake of Anthocyanidins and Their Food Sources in the European Prospective Investigation into Cancer and Nutrition (EPIC) Study. *Br. J. Nutr.* **2011**, *106*, 1090–1099.
- (16) Dieterle, F.; Ross, A.; Schlotterbeck, G.; Senn, H. Probabilistic Quotient Normalization as Robust Method to Account for Dilution of Complex Biological Mixtures. Application in  $^1\text{H}$  NMR Metabonomics. *Anal. Chem.* **2006**, *78*, 4281–4290.
- (17) Preiss, D.; Rankin, N.; Welsh, P.; Holman, R. R.; Kangas, A. J.; Soyninen, P.; Würtz, P.; Ala-Korpela, M.; Sattar, N. Effect of Metformin Therapy on Circulating Amino Acids in a Randomized Trial: The CAMERA Study. *Diabetic Med.* **2016**, *33*, 1569–1574.
- (18) Rasmussen, L. G.; Winning, H.; Savorani, F.; Ritz, C.; Engelsen, S. B.; Astrup, A.; Larsen, T. M.; Dragsted, L. O. Assessment of Dietary Exposure Related to Dietary GI and Fibre Intake in a Nutritional Metabolomic Study of Human Urine. *Genes Nutr.* **2012**, *7*, 281–293.
- (19) Jokioja, J.; Linderborg, K. M.; Kortensniemi, M.; Nuora, A.; Heinonen, J.; Sainio, T.; Viitanen, M.; Kallio, H.; Yang, B. Anthocyanin-Rich Extract from Purple Potatoes Decreases Postprandial Glycemic Response and Affects Inflammation Markers in Healthy Men. *Food Chem.* **2019**, *310*, 125797.
- (20) Clark, J. B.; Palmer, C. J.; Shaw, W. N. The Diabetic Zucker Fatty Rat. *Proc. Soc. Exp. Biol. Med.* **1983**, *173*, 68–75.
- (21) Sarikaphuti, A.; Nararatwanchai, T.; Hashiguchi, T.; Ito, T.; Thaworanunta, S.; Kikuchi, K.; Oyama, Y.; Maruyama, I.; Tancharoen, S. Preventive Effects of *Morus Alba* L. Anthocyanins on Diabetes in Zucker Diabetic Fatty Rats. *Exp. Ther. Med.* **2013**, *6*, 689–695.
- (22) Linderborg, K. M.; Salo, J. E.; Kalpio, M.; Vuorinen, A. L.; Kortensniemi, M.; Grünari, M.; Viitanen, M.; Yang, B.; Kallio, H. Comparison of the Postprandial Effects of Purple-Fleshed and Yellow-Fleshed Potatoes in Healthy Males with Chemical Characterization of the Potato Meals. *Int. J. Food Sci. Nutr.* **2016**, *67*, 581–591.
- (23) Belwal, T.; Nabavi, S.; Nabavi, S.; Habtemariam, S. Dietary Anthocyanins and Insulin Resistance: When Food Becomes a Medicine. *Nutrients* **2017**, *9*, 1111.
- (24) Zhang, L.; Dong, M.; Guangyong Xu, G.; Yuan Tian, Y.; Tang, H.; Wang, Y. Metabolomics Reveals That Dietary Ferulic Acid and Quercetin Modulate Metabolic Homeostasis in Rats. *J. Agric. Food Chem.* **2018**, *66*, 1723–1731.
- (25) Pizarro, M.; Balasubramanian, N.; Solís, N.; Solar, A.; Duarte, I.; Miquel, J. F.; Suchy, F. J.; Trauner, M.; Accatino, L.; Ananthanarayanan, M.; Arrese, M.; de Gastroenterología, D. Bile Secretory Function in the Obese Zucker Rat: Evidence of Cholestasis and Altered Canalicular Transport Function. *Gut* **2004**, *53*, 1837–1843.
- (26) Alexandre de Artiñano, A.; Miguel Castro, M. Experimental Rat Models to Study the Metabolic Syndrome. *Br. J. Nutr.* **2009**, *102*, 1246–1253.
- (27) Guo, X.; Li, H.; Xu, H.; Woo, S.; Dong, H.; Lu, F.; Lange, A. J.; Wu, C. Glycolysis in the Control of Blood Glucose Homeostasis. *Acta Pharm. Sin. B* **2012**, *2*, 358–367.
- (28) Shulman, G. I. Unraveling the Cellular Mechanism of Insulin Resistance in Humans: New Insights from Magnetic Resonance Spectroscopy. *Physiology* **2004**, *19*, 183–190.
- (29) Crawford, S. O.; Hoogeveen, R. C.; Brancati, F. L.; Astor, B. C.; Ballantyne, C. M.; Schmidt, M. I.; Young, J. H. Association of Blood Lactate with Type 2 Diabetes: The Atherosclerosis Risk in Communities Carotid MRI Study. *Int. J. Epidemiol.* **2010**, *39*, 1647–1655.
- (30) Lü, L.; Li, J.; Yew, D. T.; Rudd, J. A.; Mak, Y. T. Oxidative Stress on the Astrocytes in Culture Derived from a Senescence Accelerated Mouse Strain. *Neurochem. Int.* **2008**, *52*, 282–289.
- (31) Yang, H.; Pang, W.; Lu, H.; Cheng, D.; Yan, X.; Cheng, Y.; Jiang, Y. Comparison of Metabolic Profiling of Cyanidin-3-O-Galactoside and Extracts from Blueberry in Aged Mice. *J. Agric. Food Chem.* **2011**, *59*, 2069–2076.
- (32) Rawat, A.; Misra, G.; Saxena, M.; Tripathi, S.; Dubey, D.; Saxena, S.; Aggarwal, A.; Gupta, V.; Khan, M. Y.; Prakash, A.  $^1\text{H}$  NMR Based Serum Metabolic Profiling Reveals Differentiating Biomarkers in Patients with Diabetes and Diabetes-Related Complication. *Diabetes Metab. Syndr.: Clin. Res. Rev.* **2019**, *13*, 290–298.
- (33) Ruan, Z.; Yang, Y.; Zhou, Y.; Wen, Y.; Ding, S.; Liu, G.; Wu, X.; Liao, P.; Deng, Z.; Assaad, H.; Wu, G.; Yin, Y. Metabolomic Analysis of Amino Acid and Energy Metabolism in Rats Supplemented with Chlorogenic Acid. *Amino Acids* **2014**, *46*, 2219–2229.
- (34) Mahendran, Y.; Cederberg, H.; Vangipurapu, J.; Kangas, A. J.; Soyninen, P.; Kuusisto, J.; Uusitupa, M.; Ala-Korpela, M.; Laakso, M. Glycerol and Fatty Acids in Serum Predict the Development of Hyperglycemia and Type 2 Diabetes in Finnish Men. *Diabetes Care* **2013**, *36*, 3732–3738.
- (35) Lian, K.; Du, C.; Liu, Y.; Zhu, D.; Yan, W.; Zhang, H.; Hong, Z.; Liu, P.; Zhang, L.; Pei, H.; Zhang, J.; Gao, C.; Xin, C.; Cheng, H.; Xiong, L.; Tao, L. Impaired Adiponectin Signaling Contributes to Disturbed Catabolism of Branched-Chain Amino Acids in Diabetic Mice. *Diabetes* **2015**, *64*, 49–59.
- (36) McGarry, J. D. Dysregulation of Fatty Acid Metabolism in the Etiology of Type 2 Diabetes. *Diabetes* **2002**, *51*, 7–18.
- (37) Jawad, A. H.; Ibrahim, A. E.; Alsayed, R.; Hallab, Z. S.; Al-qaisi, Z. Study the Impact of Glucose-6-Phosphatase Activity in Type 2 Diabetic Patients and Non Diabetic Counterparts. *Preprints* **2016**, *137*, 1–6.
- (38) Kalembe, K. M.; Wang, Y.; Xu, H.; Chiles, E.; McMillin, S. M.; Kwon, H.; Su, X.; Wondisford, F. E. Glycerol Induces G6pc in Primary Mouse Hepatocytes and Is the Preferred Substrate for Gluconeogenesis Both in Vitro and in Vivo. *J. Biol. Chem.* **2019**, *294*, 18017–18028.
- (39) Hemmerle, H.; Burger, H.-J.; Below, P.; Schubert, G.; Rippel, R.; Schindler, P. W.; Paulus, E.; Herling, A. W. Chlorogenic Acid and Synthetic Chlorogenic Acid Derivatives: Novel Inhibitors of Hepatic Glucose-6-Phosphate Translocase. *J. Med. Chem.* **1997**, *40*, 137–145.
- (40) Sakamoto, K.; Holman, G. D. Emerging Role for AS160/TBC1D4 and TBC1D1 in the Regulation of GLUT4 Traffic. *Am. J. Physiol.: Endocrinol. Metab.* **2008**, *295*, E29–E37.
- (41) Szekeres, F.; Chadt, A.; Tom, R. Z.; Deshmukh, A. S.; Chibalin, A. V.; Björnholm, M.; Al-Hasani, H.; Zierath, J. R. The Rab-GTPase-Activating Protein TBC1D1 Regulates Skeletal Muscle Glucose Metabolism. *Am. J. Physiol.: Endocrinol. Metab.* **2012**, *303*, E524–E533.
- (42) Chen, L.; Chen, Q.; Xie, B.; Quan, C.; Sheng, Y.; Zhu, S.; Rong, P.; Zhou, S.; Sakamoto, K.; MacKintosh, C.; Wang, H. Y.; Chen, S. Disruption of the AMPK-TBC1D1 Nexus Increases Lipogenic Gene Expression and Causes Obesity in Mice via Promoting IGF1 Secretion. *Proc. Natl. Acad. Sci. U.S.A.* **2016**, *113*, 7219–7224.
- (43) Tsuda, T.; Horio, F.; Uchida, K.; Aoki, H.; Osawa, T. Dietary Cyanidin 3-O- $\beta$ -D-Glucoside-Rich Purple Corn Color Prevents Obesity and Ameliorates Hyperglycemia in Mice. *J. Nutr.* **2003**, *133*, 2125–2130.
- (44) Yan, F.; Zheng, X. Anthocyanin-Rich Mulberry Fruit Improves Insulin Resistance and Protects Hepatocytes against Oxidative Stress during Hyperglycemia by Regulating AMPK/ACC/MTOR Pathway. *J. Funct. Foods* **2017**, *30*, 270–281.
- (45) Roberts, L. D.; Koulman, A.; Griffin, J. L. Towards Metabolic Biomarkers of Insulin Resistance and Type 2 Diabetes: Progress from the Metabolome. *Lancet Diabetes Endocrinol.* **2014**, *2*, 65–75.
- (46) Chen, S.; Akter, S.; Kuwahara, K.; Matsushita, Y.; Nakagawa, T.; Konishi, M.; Honda, T.; Yamamoto, S.; Hayashi, T.; Noda, M.; Mizoue, T. Serum Amino Acid Profiles and Risk of Type 2 Diabetes among Japanese Adults in the Hitachi Health Study. *Sci. Rep.* **2019**, *9*, 7010.

(47) Comar, J. F.; De Oliveira, D. S.; Bracht, L.; Kemmelmeier, F. S.; Peralta, R. M.; Bracht, A. The Metabolic Responses to L-Glutamine of Livers from Rats with Diabetes Types 1 and 2. *PLoS One* **2016**, *11*, e0160067.

(48) Greenfield, J. R.; Sadaf Farooqi, I.; Keogh, J. M.; Henning, E.; Habib, A. M.; Blackwood, A.; Reimann, F.; Holst, J. J.; Gribble, F. M. Oral Glutamine Increases Circulating GLP-1, Glucagon and Insulin Levels in Lean, Obese and Type 2 Diabetic Subjects. *Am. J. Clin. Nutr.* **2015**, *89*, 106–113.